Polymeric Materials Formed by Precipitation with a Compressed Fluid Antisolvent

David J. Dixon and Keith P. Johnston
Dept. of Chemical Engineering, University of Texas at Austin, Austin, TX 78712

Roland A. Bodmeier
College of Pharmacy, University of Texas at Austin, Austin, TX 78712

Polymer microspheres and fibers are formed with a versatile new process, precipitation with a compressed fluid antisolvent. By spraying a 1 wt. % polystyrene in toluene solution into CO_2 through a 100-μm nozzle, microspheres are formed with diameters from 0.1 to 20 μm as the CO_2 density decreases from 0.86 to 0.13 g/cm^3. The uniform submicron spheres produced at high CO_2 density are due in part to the rapid atomization produced by the large inertial and low interfacial forces. Fibers, with and without microporosity, are obtained at higher polymer concentrations where viscous forces stabilize the jet. The effect of CO_2 density and temperature on the size, morphology and porosity of the resulting polymeric materials is explained in terms of the phase behavior, spray characteristics, and the depression in the glass transition temperature.

Introduction

Polymer microspheres and microcellular foams are characterized by length scales on the order of 1-10 μm or less, thousands of times smaller than found in conventional foams. Polymer microspheres are of interest as stationary phases in chromatography, as adsorbents and catalyst supports, as well as drug delivery systems. Microcellular foams are of interest as membranes, filters, porous electrodes, and insulation. A versatile technique for forming microspheres, membranes, and microcellular foams is thermally induced phase separation (Lloyd et al., 1990, 1991; Tsai and Torkelson, 1990; Aubert and Sylwester, 1991). In this technique, a liquid polymer solution is cooled rapidly into a binodal or spinodal region until the polymer is vitrified. Even larger degrees of supersaturation may be obtained with pressure by rapid expansion from supercritical solution (RESS) (Krukonis, 1984; Matson et al., 1987; Tom and Debenedetti, 1991b; Lele and Shine, 1991). Because the fluid expands over 100 bar in less than 1 ms, the high degree of supersaturation can lead to submicron particles (Debenedetti, 1990). Another promising technique for producing microcellular foams is to heat polymers containing dissolved CO_2 to nucleate small and uniform voids (Colton and Suh, 1987).

We propose a new process for forming microspheres, fibers and microcellular foams in which a liquid polymer solution is sprayed into a vessel containing compressed CO_2. Carbon dioxide is an antisolvent which diffuses into the solution and dissolves the liquid solvent to precipitate the polymer. This process is designated precipitation with a compressed fluid antisolvent (PCA). There are two boundary conditions for this process at atmospheric pressure: spray drying into a gas (at low pressure) and precipitation with a liquid antisolvent. PCA has the potential to be extremely versatile as the properties of CO_2 may be adjusted over a continuum throughout the gaseous, supercritical and liquid states. Our objective is to show how this adjustability of the density, chemical potential and transport properties of CO_2 may be utilized to control the size and morphology of the precipitated polymer. We discuss the production of polymer microspheres and fibers with controlled diameters, even in the submicron range, and evaluate the effects of temperature, density, and feed concentration. In the last section, we consider the addition of small amounts of CO_2 to the polymer solution before spraying in order to form porous materials. The implications of the depression in the glass transition temperature (T_g) of the polymer caused by dissolved CO_2 (Chiou et al., 1985; Wissinger and Paulaitis, 1991a,b; Condo et al., 1991) will be examined.

Correspondence concerning this article should be addressed to K. P. Johnston.

In an earlier antisolvent process, CO_2 is bubbled into a liquid solution to precipitate organic crystals. Gaseous CO_2 is quite soluble in a number of organic solvents at pressures from 10 to 100 bar. As CO_2 mixes with the liquid phase, it decreases the cohesive energy density (solvent strength) substantially, thus precipitating dissolved solutes. Gaseous antisolvents may be used to reduce the lower critical solution temperature (LCST) of polymer solutions to concentrate polymers (McHugh and Guckes, 1985; Seckner et al., 1988). Gallagher et al. (1989) demonstrated that the rate of addition of a gas antisolvent may be programmed to control crystal morphology, size, and size distribution over a wide range. Chang and Randolph (1990) observed that the solubilities of β-carotene and acetaminophen in liquid solvents, which were expanded with CO_2, could be varied significantly with pressure. Dixon and Johnston (1991) developed an expanded-liquid molecular thermodynamic model to predict the solubilities of pure solids in a liquid expanded in a gaseous antisolvent. This predictive model was used successfully to bridge the region between a nearly ideal liquid solution and a highly nonideal compressed fluid mixture. They also studied fractional crystallization with this technique. Although these studies provided insight into solubilities of low molecular weight substances, they did not consider the formation of polymer particles and fibers.

Two important beneficial features of supercritical fluid technology, particularly PCA, are: the environmentally acceptable nature of CO_2 compared with volatile organic solvents and the adjustability of the properties of supercritical fluids. CO_2 ($T_c = 31.05°C$, $P_c = 73.8$ bar) is a desirable solvent since it is nonflammable, relatively nontoxic, and inexpensive. For a supercritical fluid solvent, pressure and temperature may be used to adjust the solvent strength over a wide range to influence molecular interactions and phase equilibria (McHugh and Krukonis, 1989; Johnston et al., 1989). Transport rates, such as the rate of polymer swelling or solvent desorption, are accelerated for a small linear molecule such as CO_2 compared with a conventional liquid solvent (Fleming and Koros, 1986; Berens and Huvard, 1989).

To date, most studies of polymer-supercritical fluid systems have focused on separation processes, that is, polymer fractionation, extraction of impurities from polymers and regeneration of polymeric adsorbents (Daneshvar and Gulari, 1989; Shim and Johnston, 1989, 1991a,b; Meilchen et al., 1991; Watkins et al., 1991; Chen and Radosz, 1991). Another important application is the recently commercialized UNICARB process for spray painting and coating with CO_2 as the diluent, substituting for alkanes (Lee et al., 1990). The CO_2 evaporates rapidly leaving a very uniform film on the surface, and the volatile organic carbon emissions are reduced by approximately 2/3. CO_2 can reduce the viscosity of a polymer solution markedly (Garg et al., 1991). Müller and Fischer (1989) described a process for impregnating drugs into polymers, specifically polylacticacid. The polymer solution was contacted countercurrently with supercritical carbon dioxide. Another environmental application is the new propellant system called "Polygas" consisting of CO_2 in a microporous polymer with small amounts of acetone as a carrier (O'Sullivan, 1992). Processing with CO_2 will not contribute additionally to the greenhouse effect because it is easy to recover and recycle, and the CO_2 is derived from industrial processes which typically already vent it to the atmosphere.

Overview of spray processes involving compressed gases and fluids

In the PCA process, a polymer solution is sprayed through a capillary tube into a vessel containing a compressed fluid antisolvent. The fluid is chosen such that it has partial or full miscibility with the solvent, but yet it does not dissolve the polymer. CO_2 is an excellent example of such a fluid. As the solvent diffuses into the CO_2 and the CO_2 diffuses into the sprayed solution, the polymer precipitates.

The PCA process is illustrated along with the RESS and UNICARB processes on a schematic ternary diagram at constant temperature and pressure, as shown in Figure 1. In this example, the solvent and fluid are fully miscible, although this is not necessary. Also, the polymer and CO_2 are partially miscible with very limited solubility of the polymer in CO_2. Indeed, the solubility of nearly all polymers in CO_2 even at 50°C and 300 bar is quite low (Heller et al., 1985; McHugh and Krukonis, 1986; Tom and Debenedetti, 1991a). The polymer is a glass in the region as indicted schematically. The glass may be liquefied by sorption of solvent, fluid (such as CO_2), or a mixture of the two. The shape of the lower boundary of the glassy region is unknown.

Consider the mass-transfer pathway for the RESS process. Only the initial temperature and pressure are shown, as both properties decrease during expansion, so that a rigorous graphical representation would require a four dimensional diagram. In RESS, the fluid evaporates very rapidly, in less than 1 ms, and the resulting polymer microspheres, fibers, or films vitrify as the pathway intersects T_g. An important factor, which is not illustrated in the diagram, is that the size of the binodal and glassy regions vary with pressure and temperature. The major difference for the UNICARB process compared with RESS is that the initial polymer concentration is much higher, often by a few orders of magnitude. In the nozzle, CO_2 expands more rapidly than the liquid solvent, and a wet film containing

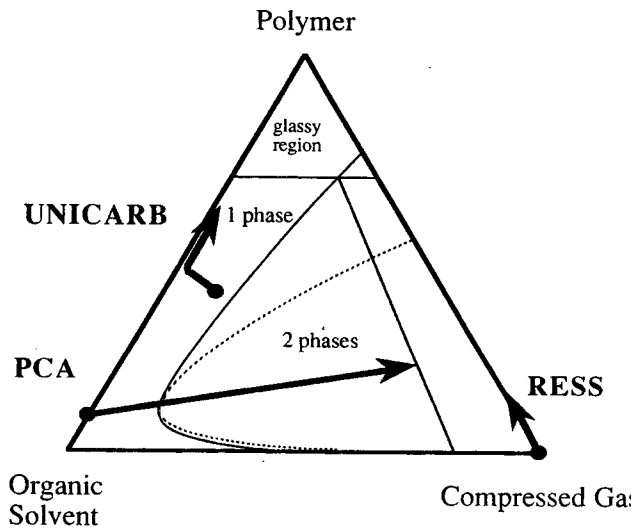

Figure 1. Schematic ternary diagram comparing pathways for various compressed fluid spray processes.

For the PCA process, pressure and temperature are constant; for the others, pressure and temperature decrease. (___ binodal curve; ____. spinodal curve).

the solvent and a small amount of CO_2 is deposited on a surface.

There are fundamental differences among the RESS, UNICARB, and PCA spray processes as shown in Figure 1. In both the RESS and UNICARB processes, the solution loses fluid, such as CO_2, during the expansion, whereas in PCA, CO_2 diffuses into the droplet during spraying. In PCA, the pathway moves to the right as CO_2 is added to the solution. The pathway enters into the two-phase region crossing a series of tie lines. Eventually, the polymer-rich side of a tie line intersects the glassy region, and the morphology is frozen in. The feed solution does not need to contain CO_2; this is the case in most examples shown. For the PCA process, the description of the thermodynamics is somewhat simpler than for the other two processes, because the temperature and pressure in the spray are relatively constant. An organic solvent is still present (unlike RESS), but it may be recovered and recycled easily. A major advantage of the PCA process vs. RESS is the lower pressures, typically 5–100 bar. A significant limitation of RESS is the extremely low solubility of most polymers in CO_2, but fluids with higher critical temperatures (Petersen et al., 1987; Lele and Shine, 1991) or CO_2 with cosolvents (Tom and Debenedetti, 1991a) may overcome this problem. In PCA, a variety of organic solvents may be used to dissolve the polymer. Many of these solvents are sufficiently miscible with CO_2 for the purposes of inducing precipitation during spraying (Francis, 1954). The use of a compressed fluid antisolvent, such as CO_2, is advantageous compared with a liquid antisolvent from the standpoint of solvent and antisolvent recovery, drying of the polymer, and environmental acceptability. Clearly, the RESS, UNICARB, and PCA precipitation processes are quite different and complementary.

Theory of Precipitation with a Compressed Fluid Antisolvent

A basic framework will be presented to help interpret the experimental studies of particle formation by PCA. While the actual mechanism of the precipitation is complex due to the interplay of thermodynamic, mass transfer and hydrodynamic effects, some insight can be gained by examining the influence of CO_2 density, system temperature and polymer concentration. It is instructive to examine previous studies of polymer foaming and gelation at ambient pressure. Aubert and Sylwester (1991) produced microporous polystyrene foams from liquid solvents using thermally induced phase separation. The morphology of open-celled polystyrene foams with pore sizes in the 1 μm range was well controlled, because the experiments were designed strategically to take advantage of the various regions in the phase diagram.

It should also be possible to exploit the phase diagram to manipulate and control morphology of polymers produced by antisolvent precipitation. A proposed schematic phase diagram relevant to PCA is shown in Figure 2, based on previous studies of precipitation with a liquid antisolvent (Koenhen et al., 1977; Yilmaz and McHugh, 1986; Pinnau, 1991). The binodal (coexistence) region is bounded with a solid curve, and the spinodal is shown by a dashed line.

A series of paths on the phase diagram is considered in Figure 2. Each path on the phase diagram represents the change in composition with time at a particular location in the sprayed droplet, or alternatively, at a given time, the change from the

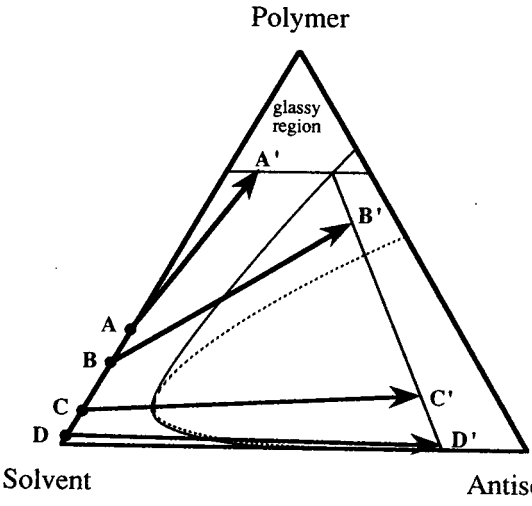

Figure 2. Schematic ternary diagram showing different precipitation schemes with a compressed fluid antisolvent.

(___ binodal curve; ____. spinodal curve).

center of the droplet to the interface with the continuous phase. After forming a polymer structure, it is necessary to freeze in the structure to preserve it. In each of the paths to be considered, the polymer morphology will become fixed when the polymer composition reaches the glassy region.

In path A-A′, the solvent evaporates into CO_2, and too little CO_2 is present to enter the binodal region. When the polymer becomes sufficiently dry, it vitrifies as a dense nonporous particle. Path B-B′ is on the polymer-rich side of the critical point and enters the binodal region, but not the spinodal. Consequently, solvent voids will nucleate and grow in the polymer phase until vitrification at B′. The closer B′ is to the antisolvent vertex, the greater the number of CO_2 voids in the polymer. Path C-C′ enters the spinodal region shortly after crossing the binodal. The spinodal region is characterized by the presence of bicontinuous phases, often with fine structure, rather than discrete droplets usually associated with nucleation and growth. Spinodal decomposition results in bicontinuous phases if the volume fraction of the polymer is high enough for the polymer coils to overlap in solution (Aubert and Sylwester, 1991). During the time between the onset of spinodal decomposition and vitrification, the structure can undergo coarsening (or ripening) from diffusional processes. Path D-D′ is on the polymer-lean side of the phase diagram, so that polymer will nucleate and grow within a solvent continuous phase.

In may cases considered below, the solvent and antisolvent will be fully miscible. The interfacial tension between pure toluene and pure CO_2 in a miscible binary mixture is zero; however, with the addition of a third component (polystyrene), an interfacial tension is present which is composition-dependent. The Weber number (N_{We}) may be used (Lefebvre, 1989) to describe the size of droplets formed in the spray process. This dimensionless number is the ratio of inertial forces to surface tension forces and is given by:

$$N_{We} = \frac{\rho_A V^2 D}{\sigma} \tag{1}$$

where ρ_A is the antisolvent density, V is the relative velocity, D is the drop diameter, and σ is the interfacial tension. A large Weber number indicates that the deforming external forces are large compared to the reforming surface forces, thus leading to drop breakup into smaller droplets. Often in PCA, the small interfacial tension and high ambient density will lead to an extremely large N_{WE}, relative to that for a spray in a low-pressure gas. Another contributing factor to droplet breakup is the relative velocity. Typical jet velocities at 22°C in the capillary tube in this study are calculated to range from 170–660 cm/s. The Reynolds number, N_{Re}, is estimated to be 25–320. Finally, the mass-transfer driving forces at the higher pressures (CO_2 densities) are large due to the toluene-CO_2 miscibility, so that the toluene will very quickly dissolve into the CO_2 and *vice versa*, possibly aiding jet breakup. Previous work has shown that mass transfer into or out of the liquid jet can significantly affect jet stability and breakup length (Coyle et al., 1981; Burkholder and Berg, 1974).

Many early studies have shown that jet breakup length for Newtonian fluids can be related to the jet velocity and viscosity through the Weber and Reynolds numbers. For example, one form is given by (Grant and Middleman, 1966):

$$\frac{L}{d} = C\, N_{We}^{1/2}(1 + 3Z) \qquad (2)$$

where the ratio L/d is the dimensionless jet breakup length, C is a constant, and $Z = N_{We}^{1/2}/N_{Re}$ is the Ohnesorge number. The Ohnesorge number (sometimes called the viscosity group) relates viscosity to surface tension forces and can be expressed as $\mu/(\rho d\sigma)^{1/2}$. At high values of Z and N_{Re}, the jet breaks up by atomization, resulting in liquid droplets much smaller than the jet diameter. At low values of Z and N_{Re}, the jet breakup results from Rayleigh instabilities. Here, the drop diameters are of the order of the jet diameter. While the above correlation is useful for Newtonian fluids, Kroesser and Middleman (1969) suggest that it can be applied to viscoelastic fluids by giving C a functional dependence. For a given Z and N_{We}, their analysis and data show that the jet is less stable for a viscoelastic fluid than a Newtonian fluid. Also, the destabilizing effect is due more to the viscoelastic behavior of the polymer solution than the non-Newtonian shear behavior.

One of the interesting features of PCA is that the particles may be dried with CO_2, and the CO_2 may be depressurized at supercritical fluid conditions. Drying removes the solvent thoroughly, which is often a major challenge. When liquids are evaporated from a matrix, the surface tension of the shrinking droplets often collapses the matrix due to capillary forces. For a supercritical fluid, there is no surface tension, and surface forces due to adsorption are minimal, so that the structure is preserved. Indeed the world's lightest solids have been formed with critical point drying (Rangarajan and Lira, 1991).

Experimental Studies

The apparatus provides for visual observation of phase behavior and the precipitation, rapid equilibration, and collection of the precipitated microparticles. The central feature of the apparatus consisted of a 1.746-cm-ID 304 stainless steel vessel approximation 28 mL in volume, with a sapphire window, as shown in Figure 3. Details of the cell are described elsewhere

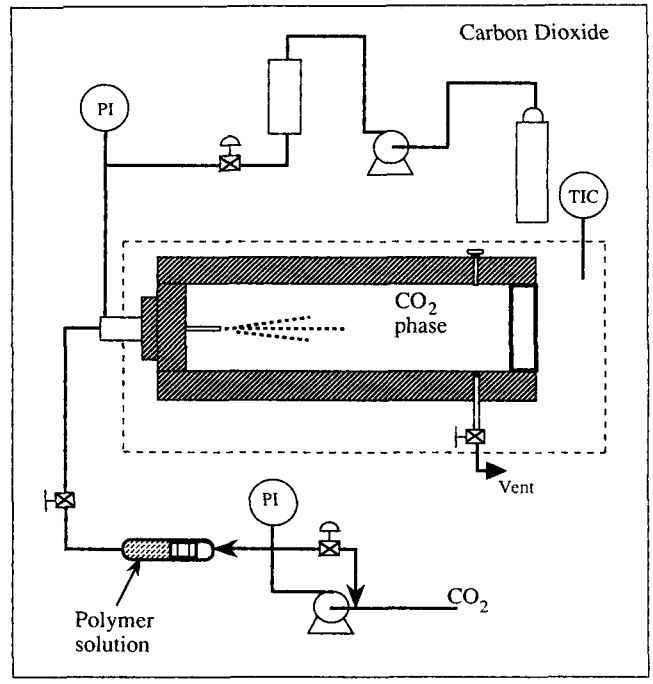

Figure 3. Apparatus for precipitation of polymer particles with a compressed fluid antisolvent.

(Johnston et al., 1989; Lemert et al., 1990). A fused silica capillary tube was used as a spray nozzle, and it was allowed to protrude slightly (~5 mm) into the back of the view cell with a total unsupported length of 11 cm. The tube was 17.4 cm long with a 100 μm inside diameter for most of this work; however, many sizes ranging from 17 μm to 150 μm were tried successfully in preliminary studies. In the future, it may be interesting to change the length of the unsupported section of the tube to determine if vibrations influence morphology, as suggested by a reviewer. The cell was optionally equipped with an oval Teflon-coated stir bar approximately 0.95 cm long by 0.48 cm diameter. Temperature was controlled to within ±0.1°C with a thermostated water bath. For CO_2 delivery, pressure was generated with a Haskel model AC-152 air-driven gas booster by compressing high-purity carbon dioxide (Liquid Carbonics UHP, 99.99%) and storing it in a 300-mL reservoir. The carbon dioxide, at controlled pressures, was metered into the view cell by a Tescom regulator (model 26-1021). The pressure in the fluid phase was measured with a Sensotec pressure transducer (TJE/7039-01 with a GM readout) to within ±0.2 bar.

The polymer solution was placed in a 2.54-cm-OD, 1.746-cm-ID stainless steel tube, with a usable volume of 36 mL (Autoclave, CNLX1608-316). The tube contained a piston with two 90-durometer buna-N o-rings. Carbon dioxide was used as the pressurizing fluid on the upstream side of the piston. The pressure was generated and controlled with a reciprocating pump (Milton Roy Minipump, model 396) and a back-pressure regulator (Tescom, model 26-1722-24-043) in a recycle loop. A low pump flow rate and a sufficiently large-volume downstream of the pump minimized the pressure fluctuations in the polymer solution. Pressure was measured to within ±0.7 bar with a bourdon tube pressure gauge. The pressure difference through the fused silica tube could be varied from a few bar

to 300 bar. For the runs described in this work, a differential pressure of 55 bar was used, unless otherwise noted. The flow rate through the capillary tube, for a given differential pressure (ΔP), was calculated by flowing the solution into a small test tube at atmospheric pressure, measuring the time allowed for flow and weighing the amount collected. It was assumed that the flow rate measured for a certain ΔP would remain constant, regardless of the discharge pressure. Increased temperature, however, will increase the flow rate by decreasing the viscosity. Estimates of the solution temperature at the capillary tube entrance were typically within 2°C of the bath temperature for the 1% polymer solution and well within 0.2°C for the 5 and 6% solutions.

The PCA experiment began by adding a polymer solution to the liquid pump. The polymer solution consisted of a polystyrene standard (Pressure Chemical, $M_W = 200{,}000$, $M_W/M_n = 1.05$) dissolved in toluene (Fisher, Certified A.C.S.). The pressure in the view cell was adjusted to within ±0.2 bar to achieve the desired density by addition of CO_2. The system was allowed to equilibrate 15–30 minutes. The valve upstream of the nozzle was opened for a short time (10–15 s) to allow the polymer solution to spray into the CO_2. An obvious cloudy, white precipitation was observed immediately as the jet entered the view cell. After the polymer precipitated, CO_2 was swept through the cell to remove the solvent. At the view cell outlet, a small needle valve (Whitey, SS-21RS4) was placed downstream of a 2-μm stainless steel frit filter and was used during purging of the cell with CO_2 and depressurization. The cell was then allowed to slowly depressurize, typically for 50 minutes. In some cases, a structured precipitate was formed. To preserve this structure, but perhaps with some shrinkage (Rangarajan and Lira, 1991), the temperature and pressure were raised above CO_2 critical conditions prior to depressurizing. A sample of the precipitated polymer was then collected for analysis either from the inside walls of the view cell or on a small glass plate, which had been inserted into the cell prior to sealing.

Another type of antisolvent experiment was performed in the same vessel with a procedure similar to that of Gallagher et al. (1989). In this experiment, a few milliliters of polymer solution were added to the view cell along with a stir bar. Carbon dioxide antisolvent was added slowly until the solution was on the verge of precipitation. Then, CO_2 was added quickly or slowly, depending on the desired particle size, to cause the polymer to precipitate. Purging and depressurization were accomplished as described above.

The microparticles and fibers were analyzed by optical microscopy (Leitz, Fluovert, Type 090-123-012), scanning transmission electron microscopy (STEM, JEOL JEM-1200EX), or scanning electron microscopy (SEM, JEOL JSM-35C). Sample preparation for the SEM consisted of mounting the polymer sample, either as a loose powder or a small piece cut from the glass plate, on a small piece of double-sided carbon-conductive tape (E. F. Fullam Co., carbon conductive double sticky tape). This tape was placed on a 0.95 cm diameter by 0.95 cm long aluminum or brass sample stage. The sample was sputter-coated with gold-palladium to an approximate thickness of 200 Å.

A 3.175-cm-OD, 1.27-cm-ID, 10.16-cm-long sapphire tube was used as a view cell to observe the capillary nozzle spray. A Nikon 35-mm camera, equipped with a strobe and a macrolense, was used to photograph the liquid jet. Control of CO_2 density and differential pressure was achieved as described above.

Results and Discussion

Effect of temperature

To examine the effect of temperature on polymer morphology, experiments were performed at constant density, not constant pressure. A number of properties are much more clearly related to density than pressure, including the viscosity, chemical potential, interfacial tension with another fluid, phase behavior, and so on (Kumar and Johnston, 1988). Although it is convenient to describe the system by the CO_2 density, one must remember that the density of the liquid solution changes throughout the spray during mass transfer.

The smallest microspheres were made by spraying a 1 wt. % polystyrene in toluene solution into CO_2 which had a density greater than 0.7 g/cm^3. Figure 4a shows a STEM photograph of these small microspheres. In this case, the temperature of the liquid CO_2 was 10°C with a density of 0.863 g/cm^3. Figures 4a and 4b show that the primary polymer microspheres are very small, on the order of 100 nm, regular in shape, and have a fairly monodisperse distribution. This suggests that the initial droplet size distribution is likewise fairly monodisperse. It is interesting that the particle size is comparable with that in RESS, which is well suited for the formation of very small, uniform particles. The microstructure is an airy, open network where the primary polymer particles have flocculated loosely but have not coalesced into larger particles. By visual inspection, we observed the macrostructure to be open, loosely connected, and subject to collapse when crushed mechanically or when subjected to the surface tension forces of a liquid-vapor meniscus during drying. The flocculated structure was observed to develop within 30 seconds after spraying.

At a constant CO_2 density of 0.86 g/cm^3, the particle size increases significantly as the temperature is increased to 30°C (Figure 4c). This trend becomes even more evident when the temperature is increased to 40°C (Figure 4d). At 40°C, the mean particle size is approximately 1 μm, representing a tenfold increase over those formed at 10°C (Figure 4a). The particles are agglomerated (fused or coalesced), and while there is still flocculation present, it is on a much smaller scale, with connected regions approximately 10–20 μm in length. The macrostructure appears as a powder instead of a "cobweb-like" open, airy floc. It is likely that the tendency for the polystyrene microspheres to flocculate has decreased at the increased temperatures (Napper, 1983; Hiemenz, 1986).

The agglomeration may perhaps be enhanced by plasticization of the polymer due to a depression in the glass transition temperature (T_g). The T_g can be depressed significantly, although few data are available above 10 bar (Chiou et al., 1985; Wissinger and Paulaitis, 1991a,b). Condo et al. (1992) predicted a new retrograde vitrification phenomenon where a liquid to glass transition occurs with increasing temperature. CO_2 can plasticize certain polymers rapidly, because of its rapid diffusion. In the plasticized polymer, diffusion coefficients of other solutes or solvents can be accelerated by several orders of magnitude (Berens and Huvard, 1989).

Figures 5a and 5b are SEM photographs which show that

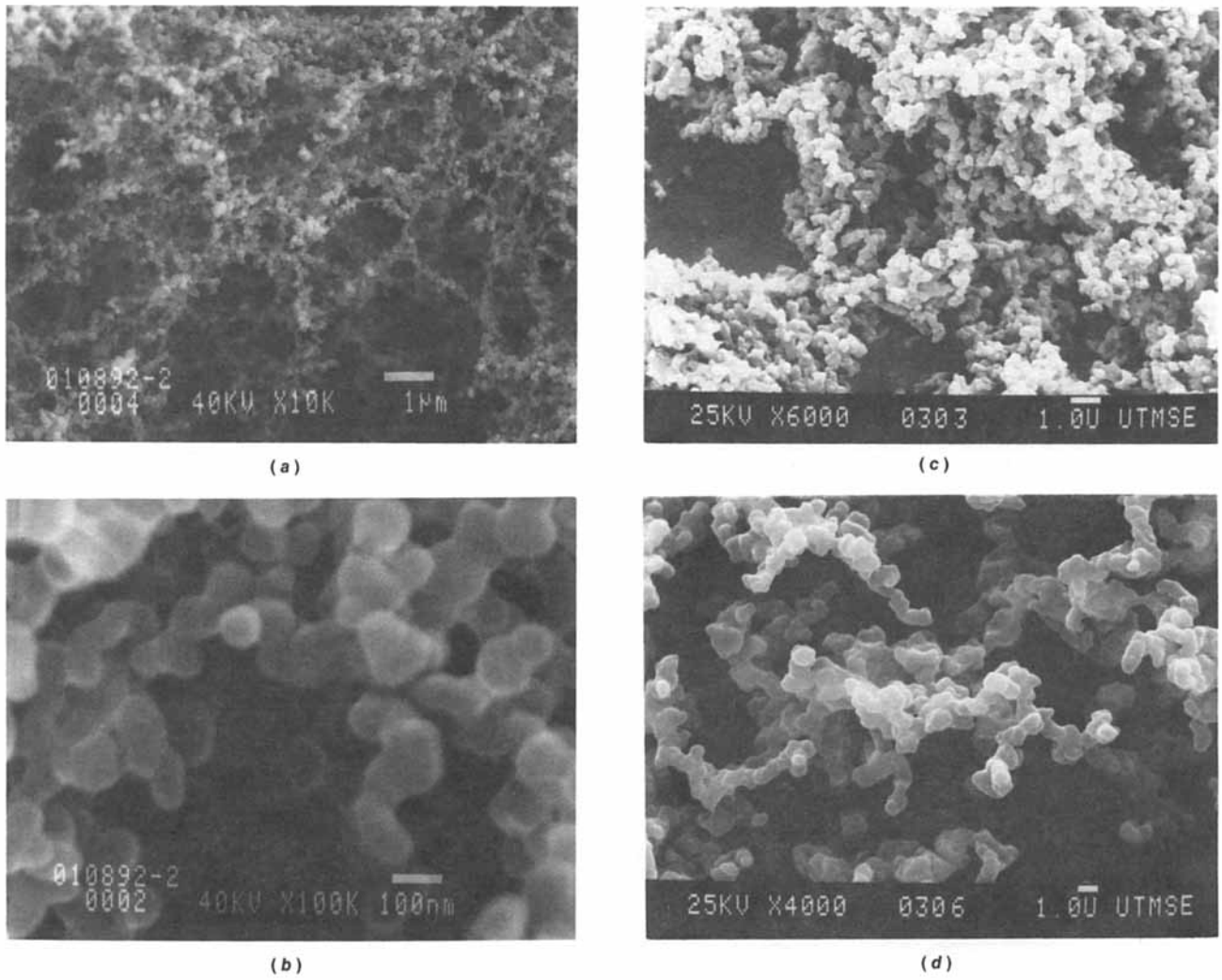

Figure 4. Polystyrene microspheres formed by spraying a 1% polystyrene in toluene solution through a 100-μm nozzle into CO_2.

0.86 g/cm^3; a) & b) 10°C and 45.8 bar (STEM); c) 30°C and 133.7 bar (SEM); d) 40°C and 224.7 bar (SEM).

the fine structure can also be produced at room temperature. These particles were made at slightly lower densities (0.778 g/cm^3), and again the microspheres were on the order of 100 nm diameter. Figure 5a gives a good perspective of the airy "cobweb-like" macrostructure which occurs for these small polystyrene microspheres. Figure 5b is a close-up showing details of the fine microstructure (similar to Figure 4a). Increasing the temperature to 40°C (Figure 5c) results in larger particles, loss of the macroscopic flocculated structure, and modest agglomeration, consistent with the above results.

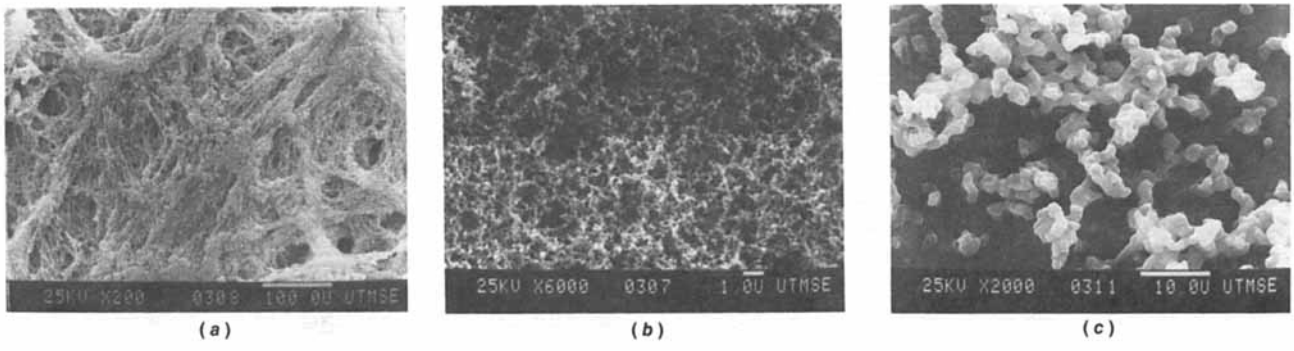

Figure 5. SEM of polystyrene microspheres formed by spraying a 1% polystyrene in toluene solution through a 100-μm nozzle into CO_2.

0.778 g/cm^3; a) 25°C and 80.3 bar; b) 20°C and 58.6 bar; c) 40°C and 148.2 bar.

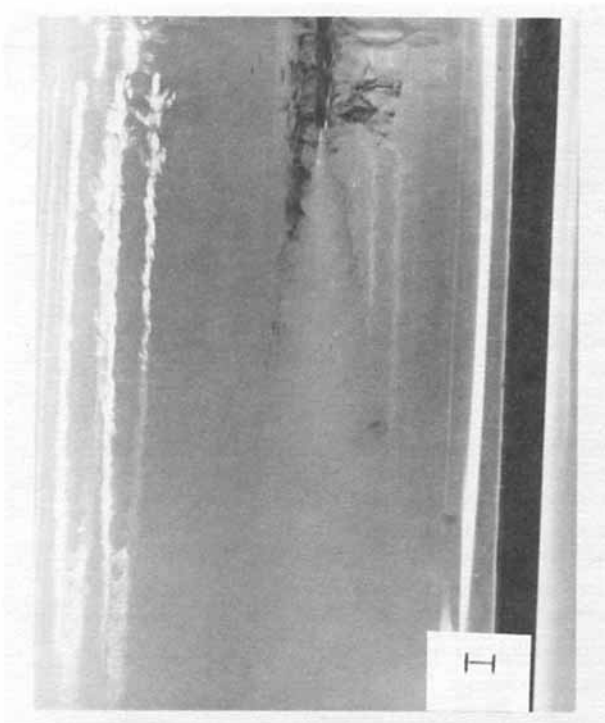

Figure 6. Atomization of a 1% polymer solution sprayed from a 100-μm ID nozzle (358 μm OD) into CO_2 at 22°C and 0.74 g/cm^3.

Scale bar is 1 mm.

It was observed that the spray atomized extremely close to the capillary nozzle to form very small droplets, which may explain the submicron size of the precipitated microspheres. Figure 6 shows qualitatively how rapidly a 1% polystyrene solution atomizes when sprayed into dense (0.74 g/cm^3) liquid CO_2. As a reference, the scale bar in the background has 1 mm minor divisions, and the capillary tube is 0.358 mm OD by 0.100 mm ID. As the photograph shows, the jet atomizes almost immediately into very fine droplets. The small size of the droplets may be expected because of the large density of the continuous phase (CO_2), high jet velocity (655 cm/s), and low interfacial tension. For comparison, if the same solution is sprayed into CO_2 vapor (~0.2 g/cm^3) at the same temperature and ΔP through the tube, we observe that the liquid jet does not atomize immediately, but its breakup is delayed a few millimeters, resulting in droplet diameters on the order of the initial jet diameter. Obviously the jet breakup mechanism is sensitive to the hydrodynamic interactions with the CO_2 over this broad density range.

The fast diffusion of CO_2 into and toluene out of the liquid polymer droplet will cause rapid precipitation followed by freezing of the morphology, as the polymer-rich phase passes through the vitrification point. For the experiment shown in Figures 4a and 4b, this vitrification is sufficiently rapid to preserve the very small microspheres. How fast the polymer vitrifies is a function of the mass-transfer driving forces. For these liquid CO_2 conditions, toluene and CO_2 are fully miscible so that there is a large driving force for toluene to transfer into the CO_2 phase and *vice versa*.

Although the mechanism for the formation of the above polymer structures is not yet known, it is instructive to examine several possible scenarios.

1. In this case, a drop comprising the polymer solution collapses and forms a single microparticle. Knowing the polymer concentration and assuming that the polymer collapses to a single sphere at its normal density (for polystyrene, ~1.05 g/cm^3) it is easy to estimate the initial droplet diameter from the final polymer microsphere diameter. For a 1% polystyrene solution the final polymer diameter will be ~20% of the original liquid droplet size. Thus for a 0.5-μm liquid droplet, the expected polymer diameter would be 100 nm (as in Figure 4b), and the particle would contain approximately 1,600 individual polymer chains. It is quite possible that atomization of the liquid jet could produce 0.5-μm liquid droplets.

2. A single liquid drop could lead to multiple polymer microparticles. Here, more than one nucleation site would be present in each drop and growth could occur by diffusion of polymer chains to the nucleation sites as well as by interaction (coalescence) between growing nuclei. The evaporation of toluene and shrinkage of the drops will facilitate this coalescence.

3. In a liquid droplet it is possible that the compositional mass-transfer path (Figure 2) crosses the spinodal curve. However, the typical bicontinuous, interpenetrating network caused by spinodal decomposition would not be expected, due to the low polymer concentration (1%) (Aubert and Clough, 1985). We estimate that the concentration would need to be above 2 wt % polystyrene for these networks to form.

Another scenario, which may be ruled out, is as follows. If the polymer concentration is dilute enough, the individual chains may exist as discrete units without overlapping in solution. As the solvent is removed, each individual polymer chain could collapse into a single sphere. If this occurred, the expected sphere diameter would be ~8 nm, far less than observed for the 1% solutions. Again, as the liquid drops shrink, some coalescence of nuclei would likely occur.

It is premature to determine which of the above mechanisms is more likely for polymer microsphere formation based on the final sphere size alone. Unfortunately, the small liquid droplets are difficult to image in the existing high-pressure view cells, especially while in motion. However, the fact that the microspheres are small and uniform at low temperatures suggests that hydrodynamic jet breakup creates initially small and uniform droplets, while rapid mass transfer and thermodynamics explain how the small particles are formed and preserved through vitrification.

For all cases, the pressure drop across the capillary tube was constant. However, the flow rate varies with temperature. For a temperature increase from 22 to 40°C the viscosity decreases by ~35% and thus the velocity increases by the same order. With the increased velocities the N_{We} also increases. Thus, even smaller spray droplets would be expected and subsequently smaller polymer particles. However, Figures 4c and 4d show that the actual polymer particles are larger. Although the initial spray droplets are smaller, additional factors, such as agglomeration, cause the larger polymer particles. Up to 25°C the same morphology is observed, but at 30°C it begins to change, and finally at 40°C the particles are an order of magnitude larger.

To evaluate the role of agglomeration, two experiments were carried out at 22°C and 80.3 bar (Table 1). Here both experiments were conducted in exactly the same manner except that

Table 1. Observed Polymer Morphology Produced by Spraying a Polystyrene in Toluene Solution into Carbon Dioxide*

T (°C)	P (bar)	CO_2 Density (g/cm^3)	wt. % Polymer (CO_2-Free)	Primary Particle Diam. (μm)	Microstructure	Macrostructure
0.3	39.6	0.930	1	~0.1	microspheres, flocculated	cobweb-like
10	45.8	0.863	1	~0.1	microspheres, flocculated	cobweb-like
25	133.7	0.862	1	~0.1	microspheres, flocculated	cobweb-like
30	164.1	0.862	1	0.3–0.4	microspheres, sl. agglomerated	fluffy powder
35	194.4	0.862	1	~0.5–3	microspheres, agglomerated 10–20 μm**	fine powder
40	224.7	0.862	1	~0.5–3	microspheres, agglomerated 10–20 μm**	fine powder
20	58.6	0.778	1	~0.1	microspheres, flocculated	cobweb-like
25	80.3	0.778	1	~0.1	microspheres, flocculated	cobweb-like
30	102.7	0.778	1	0.2–0.4	microspheres, sl. agglomerated	fluffy powder
35	125.5	0.778	1	0.5–2	microspheres, agglomerated 10–30 μm**	fine powder
40	148.2	0.778	1	0.5–3	microspheres, agglomerated 10–50 μm**	fine powder
30	72.9	0.626	1	0.5–1	microspheres, agglomerated 20–30 μm**	fine powder
35	85.9	0.626	1	0.5–2	microspheres, agglomerated 20–50 μm**	fine powder
40	99.5	0.626	1	0.5–3	microspheres, agglomerated 30–50 μm**	fine powder
35	81.1	0.50	1	1–2	microspheres, agglomerated 10–20 μm**	fine powder
40	90.5	0.50	1	2–5	microspheres, agglomerated 10–20 μm**	fine powder
35	79.6	0.40	1	0.5–3	microspheres, agglomerated 10–30 μm**	fine powder
40	86.9	0.40	1	0.5–3	microspheres, agglomerated 10–30 μm**	fine powder
40	84.2	0.34	1		broken film, much agglomeration	film
40	81.7	0.30	1		film	film
10	44.8	0.134	1	1–100	porous microspheres, sl agglom.[‡]	powder
22	80.3	0.77	2.5	~0.1	microspheres, flocculated	cobweb-like
22	80.3	0.77	2.5	0.5–3	microspheres, agglomerated[§]	cobweb-like
22	62.4	0.74	6	20–40	fibers	fibers
22	62.4	0.74	6***	50–60	expanded fibers[†]	fibers
25	133.7	0.862	5.8[‡]	100–150	expanded fibers[+]	fibers
25	64.3	0.243	5.8[‡]	0.5–2	microspheres[+]	powder

*Unless otherwise noted the solution was sprayed through a 100 μm ID capillary tube at a constant differential pressure of 55 bar
**Agglomerated groups are in an open network
***With 5 wt.% CO_2 (based on total solution weight) added to polymer solution prior to spraying
[†]Sprayed through a 50 μm ID capillary tube
[‡]With 6 wt.% CO_2 added (based on total solution weight) to polymer solution prior to spraying
[+]ΔP across tube was 136 bar
[‡]1 min. after spraying, CO_2 was added to vitrify the polymer
[§]Same as above run except after toluene purge, raised T to ~46°C for 13 minutes and then cooled to 33°C and depressurized

in the latter experiment, after the toluene was purged, the temperature was raised to ~46°C for 13 minutes, and then the cell was cooled back down to 33°C and depressurized. The two macrostructures appeared to be similar, but the microparticles in the second experiment were larger and more agglomerated with an appearance similar to Figure 4d. It is likely the polymer was plasticized (depressed polymer T_g) by the presence of CO_2 and small amounts of toluene, which facilitated coalescence of the flocculated particles.

To explore the issue of plasticization without the presence of toluene, polystyrene spheres (of unknown molecular weight), which were made by emulsion polymerization, were subjected to dense CO_2 environments at increasing temperatures, typically for 1 hour. Without CO_2 (or other plasticizing agents) present, polystyrene will not soften until approaching the normal T_g (~105°C). At 21°C and a CO_2 density of 0.86 g/cm^3 there are no visible changes in the morphology or individuality of the spheres compared with the untreated spheres. There are still no changes at 35°C (Figure 7a). However, at 40°C (Figure 7b) polymer spheres have softened, suggesting plasticization. The regular spherical shape is not as prevalent, and some of the particles have agglomerated into groups of 2 or more. Finally, at 60°C the particles have fused into a nondescript mass. While this approach is somewhat qualitative in nature, it dramatically points out the effect of CO_2 sorption on the glass transition temperature. Clearly, this plasticization could affect the agglomeration of the primary particles markedly. There is a need for a more in-depth study to understand the lowering of T_g by sorbed gases, such as CO_2. Such a study would serve to test predictions of the behavior of liquid and glassy regions for ternary systems at different temperatures and pressures (Condo et al., 1992).

The temperature effects become more complicated in the CO_2 density region from 0.63 g/cm^3 to ~0.30 g/cm^3. At lower temperatures, such as 0–31°C, the existence of the two-phase CO_2 liquid-vapor equilibrium region causes a liquid pool to form on the bottom of the vessel. Only by operating at temperatures above or very near the CO_2 critical point can one access CO_2 densities on the order of 0.4 g/cm^3 in the one-phase region. At CO_2 densities below ~0.30 g/cm^3, we observe that changing the temperature from 0–35°C does not appear to play a major role in affecting polystyrene particle size or morphology. Above 40°C, where the polymer is plasticized, the polymer particles agglomerate and even form films (Table 1).

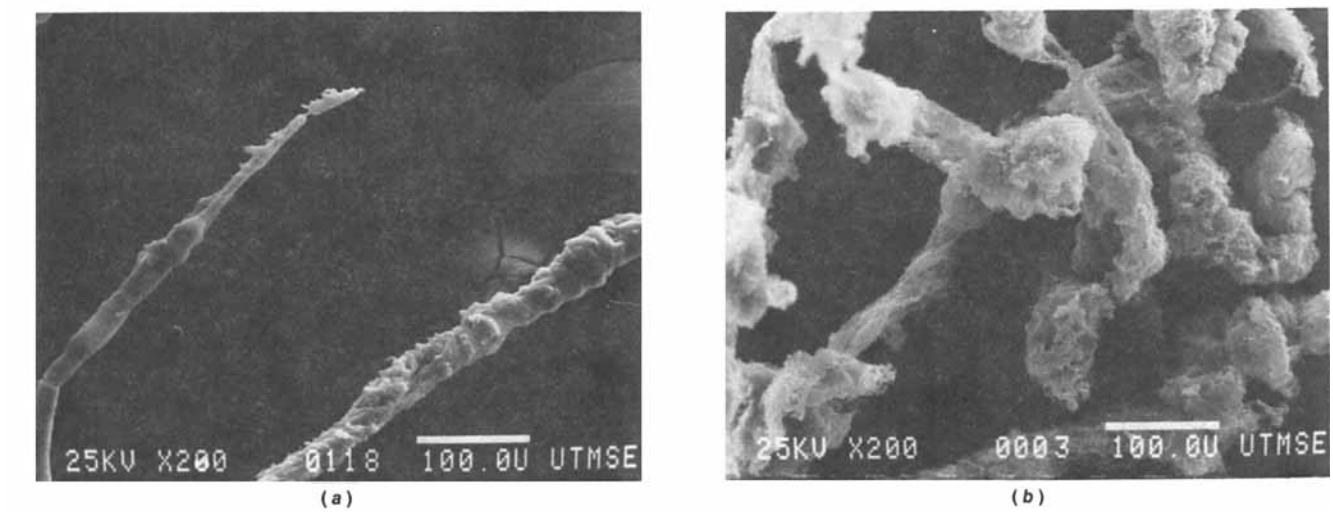

Figure 7. SEM of polystyrene spheres made by emulsion polymerization and subjected to CO_2.

a) 35°C, 0.73 g/cm^3, and 104.4 bar; b) 40°C, 0.68 g/cm^3, and 107.9 bar.

Effect of concentration

Polymer concentration is another important variable for controlling morphology. The previous results have been for 1 wt. % polystyrene in toluene. Increasing the concentration to 5 or 6% leads to fiber formation. Figure 8a (and Table 1) shows an example of polystyrene fibers formed by spraying a 6% solution into CO_2 at 22°C and a density of 0.74 g/cm^3. In contrast, for a 1% solution at approximately the same CO_2 conditions, very small microspheres are produced (Figure 5b). For a 5% or 6% polymer concentration, fibers are formed over the temperature range of 10–40°C, and for CO_2 densities of 0.86–0.57 g/cm^3.

Fibers are formed for a number of reasons. The primary reason appears to be the hydrodynamics of liquid jet breakup. In general, the viscosity of the sprayed liquid acts as a stabilizing force on the jet (see Eq. 2). Increasing the viscosity decreases the N_{Re} and also hinders the development of any natural jet instabilities, thus delaying jet disintegration (Lefebvre, 1989). For cases of constant jet velocity, if the breakup length increases, droplets will be formed later. The viscosities of the 5% and the 1% solutions at 22°C, are 0.055 g/cm/s and 0.018 g/cm/s, respectively, for a shear rate corresponding to a ΔP through the 100-μm capillary tube of 55 bar. These viscosities were calculated using the Weissenberg-Rabinowitsch equation (Bird et al., 1977). It is also noted that the viscosity of the sprayed jet will increase steadily as toluene is transferred into the continuous CO_2 phase. Because of the high viscosities, it is likely that the time scale for droplet formation is longer than the time scale for polymer precipitation, resulting in fibers rather than microspheres.

The increase in the viscoelasticity, as concentration is increased from 1 to 5%, will destabilize the jet. Clearly, the results indicate that the increase in jet stability due to viscosity dominates the viscoelastic contribution.

It is estimated that at the 1% concentration the solution is close to the dilute region (Billmeyer, 1984), where polymer

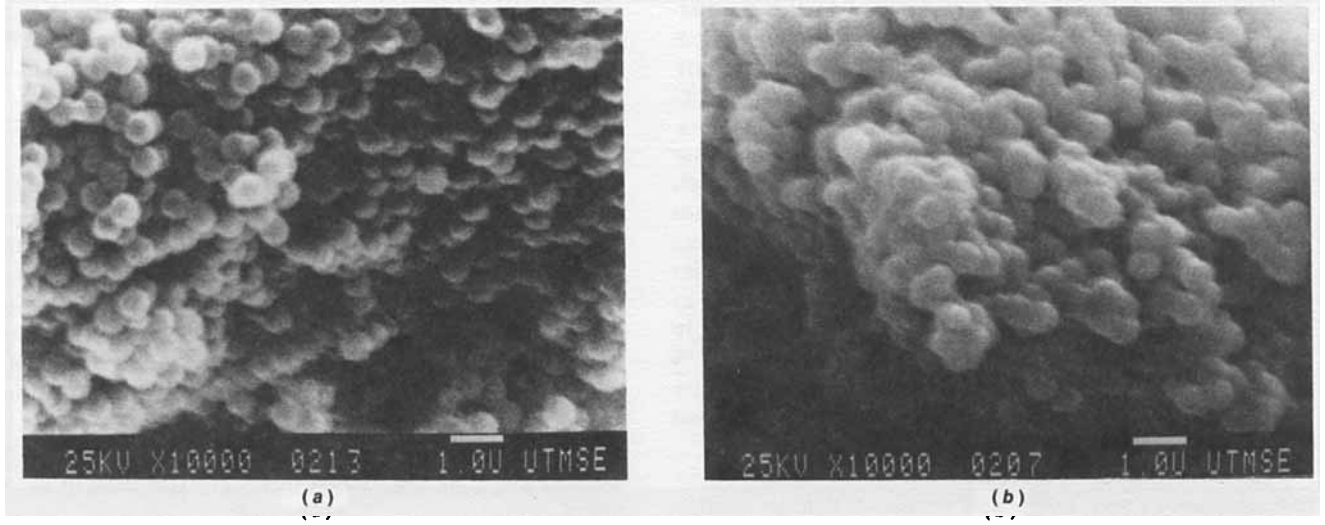

Figure 8. SEM of polystyrene fibers formed by spraying a polystyrene in toluene solution into CO_2.

22°C, 0.74 g/cm^3, and 62.4 bar; a) 6% polystyrene solution sprayed through a 100-μm nozzle; b) 6% polystyrene solution with 5% CO_2 added before spraying through a 50-μm nozzle.

chains exist in solution without overlapping. At at concentration of 5% the polymer solution falls into the semidilute region, where the polymer coils interpenetrate one another significantly. Consequently, there may be kinetic limitations as to how fast the polymer coils can untangle to form discrete spheres.

A final reason for fiber formation at higher concentrations is that less antisolvent is required to precipitate the polymer, because the solution is closer to saturation. This corresponds to shifting from path D-D′ on Figure 2 to path C-C′, where the latter path has a shorter distance from the starting point to the binodal curve. The solution will precipitate sooner as CO_2 is added, leading to a quicker vitrification or freezing-in of the final polymer morphology. For a 6% relative to a 1% polymer concentration, the faster precipitation will stabilize the liquid jet prior to its breakup, thus producing fibers instead of particles.

The mechanism for fiber formation (Figure 8a) is analogous to mechanism 1 above, except now we assume that the solution in the jet will precipitate to form a single polymer fiber. For a 100-μm jet of 6% polystyrene solution, a 22-μm solid fiber would be formed, which is consistent with the results in Figure 8a. The somewhat larger sizes in the figure may be explained by either die swell (an elastic response) or by the fact that the jet/soft-fiber velocity can vary with distance from the capillary tube exit due to interaction with the dense CO_2 phase. A section of jet which is closer to the tube exit will have a slightly higher velocity than the section which is immediately downstream. With the jet still "soft" (that is, a more viscous jet or a plasticized polymer fiber) this compression effect will cause a "bunching" or swelling of the fiber diameter. Obviously, this is one reason why extruded fibers are pulled or removed from the exit of an extruder during commercial manufacture.

This proposed mechanism differs from the mechanism for fiber production in RESS. In RESS, fiber formation depends on the location in the nozzle where the supercritical solvent density is sufficiently small to cause phase separation to occur (Lele and Shine, 1991). In PCA, the fiber formation takes place in the jet just beyond the tip of the nozzle. Thus, it may be somewhat easier to understand and control the behavior in PCA, since it is not necessary to model complex temperature, density, and solubility profiles in a nozzle.

Porous particles

Porous fibers were produced when 5 wt. % CO_2 was added to a 6 wt. % polystyrene in toluene solution and sprayed into liquid CO_2. Prior to spraying this solution was still in the one-phase region, as confirmed by visual observation in a separate phase behavior experiment in the view cell. Figure 8b shows typical porous polystyrene fibers, which were produced by spraying this solution into CO_2 at 22°C and a density of 0.74 g/cm^3. Compared with the nonporous fibers (Figure 8a), they felt softer, more flexible, had a larger diameter, and from SEM photographs, contained visible open regions. Adding CO_2 is known to reduce the viscosity of a polymer solution (Lee et al., 1990; Garg et al., 1991). This was observed experimentally, as a 6% polymer solution would not flow easily through a 50-μm capillary tube; however, with CO_2 added it flowed quite easily. Compressed gases have been added in sprays previously to aid in atomization of the liquid jet (Lefebvre, 1989); however, these studies did not consider the effect when a solute was precipitating. As the solution containing dissolved CO_2 exits the nozzle tip, the dissolved CO_2 expands rapidly, acting like a "blowing agent." It is conceivable that this rapid expansion could break up the liquid stream rather quickly; however, this did not happen as evidenced by the resultant fibers. It is likely that the rapid precipitation occurs before the jet has time to break into droplets. This observation is supported by phase equilibrium experiments which indicate that the polymer solution is already quite near phase separation, such that adding a small amount of CO_2 antisolvent (by spraying into CO_2) causes precipitation. This mechanism of producing porous fibers is somewhat related to production of microcellular foams, which can be formed by heating polymers containing dissolved CO_2 (Colton and Suh, 1987). The CO_2 expands and creates voids in the polymer which then vitrifies before the structure can collapse. The porosity of the fibers may be tailored by changing the amount of CO_2 predissolved in the solution.

Porous microspheres have been produced at 10°C by spraying a 1% polystyrene solution into low-density (0.134 g/cm^3) CO_2. In this experiment, two liquid phases were formed with the bottom phase containing the precipitated polymer phase. The mixture was allowed to agglomerate for 1 minute before liquid CO_2 was added to cause vitrification of the polymer. Figure 9 is a close-up of one of these spheres which was scraped from the view cell wall. The pore sizes are estimated to be 1–2 μm. The smaller microspheres (Table 1) are probably caused by precipitation of polystyrene during the liquid CO_2 addition cycle.

Different types of morphologies have also been obtained by dissolving CO_2 into a stirred liquid polymer solution (see Table 2). If CO_2 is added relatively fast (< 1 s), microspheres result with 1–2 μm diameters and modest agglomeration (Figure 10a). These smaller spheres do not appear to have any visible porosity, and if they do, the pore size would be estimated to be less than 100 nm. Figure 10b shows polystyrene microspheres which are 2 orders of magnitude larger, ~ 100 μm in diameter,

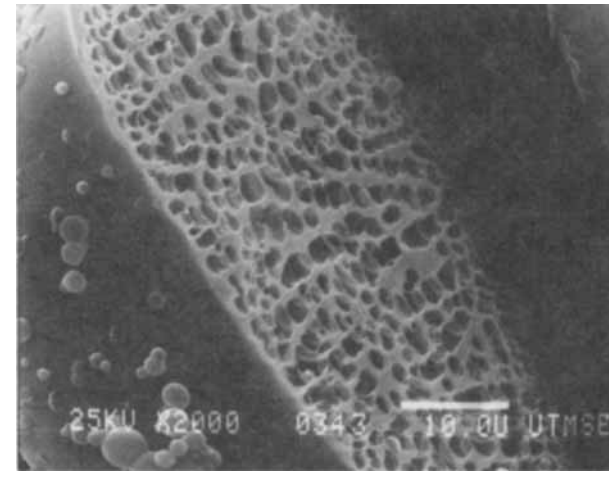

Figure 9. SEM of a porous polystyrene microsphere formed by spraying a 1% polystyrene in toluene solution through a 100-μm nozzle into CO_2 (10°C, 0.134 g/cm^3, and 44.8 bar), then adding more CO_2 after 1 min to cause vitrification.

Table 2. Polymer Morphology Produced by Rapidly Adding Carbon Dioxide to a Polystyrene in Toluene Solution While Stirring

T (°C)	Rate of CO_2 Addition (s)	wt. % Polymer	Primary Particle Diam. (μm)	Microstructure	Macrostructure
22	<1	1	1-5	microspheres, sl. agglomeration	fine powder
22	~5	1	1-100	porous microspheres, agglomerated	fine powder

containing 1-5 μm pores (as estimated by SEM). The larger spheres were made by adding CO_2 more slowly (~5 s). For a dilute 1% polymer solution it would be expected that the mechanism of precipitation would be by nucleation and growth, especially with a relatively slow addition of antisolvent. For example, the generation of supersaturation is much slower than in spray PCA leading to much larger particles compared with Figure 4a.

A plausible explanation for the pores in the larger particles is as follows. Polymer spheres are formed by nucleation and then increase in size by growth as well as agglomeration through contact with other soft spheres. Porosity could possibly occur by occlusion of the solvent phase as the spheres agglomerate. Another perhaps more likely possibility is that the solvent phase forms porous regions by nucleation and growth in the polymer-rich phase as more CO_2 is transferred into the sphere. This mechanism also can explain the porous morphology shown in Figure 9. Here, the addition of CO_2 after 1 minute would cause a rapid transfer of CO_2 into the polymer-rich phase, leading to porosity by nucleation and growth of a solvent phase. The composition starts on the polymer-rich side of the tie line and follows a path to point B′ (see Figure 2). Slow depressurization ensures that the spheres retain their porous nature without collapsing or foaming.

Effect of density

As CO_2 density is varied isothermally between 0.863 and ~0.4 g/cm^3 the resulting polymer morphology does not change significantly. This can be seen readily by comparing morphologies observed at 35°C for difference CO_2 densities and a 1% polystyrene solution (see Table 1). The primary size of the microparticles is essentially constant. The size of the floc varies slightly, mostly due to slight variations in spray times. These results suggest that the inertial forces are sufficiently strong to atomize the jet at 0.4 g/cm^3, and a further increase in density has little effect on this atomization. Also, since toluene and CO_2 are fully miscible over this density range, the thermodynamic and mass-transfer driving forces are relatively constant.

As CO_2 density is lowered below ~0.4 g/cm^3, the PCA technique is more analogous to conventional spray drying. As mentioned above, the 1% polystyrene in toluene liquid jet did not atomize at a CO_2 density of about 0.2 g/cm^3, but rather broke up into significantly larger droplets. These larger droplets could be expected to produce larger microspheres. If the liquid jet (1% polystyrene in toluene solution) broke up into drops of 50 or 100 μm in diameter, then the final polymer sphere diameter would be 10 or 20 μm, respectively, based on mechanism 1. The recovery of the resulting polymer microspheres was complicated by the formation of a second liquid phase on the bottom of the cell, which was cloudy indicating the presence of precipitated polymer. Significant agglomeration of the recovered polymer was observed, presumably due to the high concentration of toluene in the lower phase. The presence of a second liquid phase, even for the low amounts of toluene sprayed into the cell (typically 2-6 wt. % toluene in the cell), is expected based on the toluene-CO_2 phase equilibria (Ng and Robinson, 1978; Dixon and Johnston, 1991). Of course, the presence of a small amount of a third component (polystyrene) further raises the dew point pressure.

At 40°C and at CO_2 densities below 0.34 g/cm^3, polystyrene films were formed (see Table 1). These films were most likely caused by coalescence of the polymer in the toluene-rich phase.

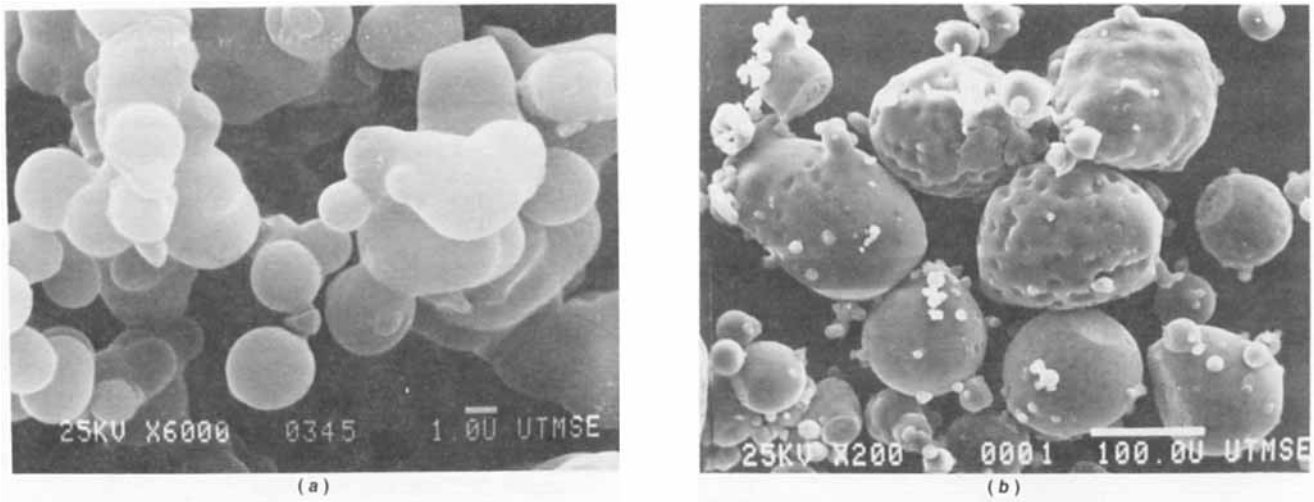

Figure 10. SEM of microspheres formed by adding CO_2 to a stirred 1% polystyrene in toluene solution at 22°C: a) rapid CO_2 addition, <1 s; b) slower CO_2 addition, ~5 s.

The next to the last entry in Table 1 shows that spraying a 5.8% polystyrene in toluene solution (to which 6% CO_2 had been added prior to spraying) into CO_2 at 25°C with a density of 0.862 g/cm^3 produced expanded fibers. However, when spraying the same solution into CO_2 vapor at only 0.24 g/cm^3 (last item in Table 1) it was observed that the liquid jet broke up into distinct droplets rather than forming fibers. Here, liquid and vapor CO_2 phases were present prior to and during spraying. By spraying into a CO_2 vapor phase and allowing the droplets to fall into a liquid CO_2 pool, the resultant particles did not agglomerate. The liquid CO_2 diluted the toluene in the precipitate and aided the vitrification of the polymer. These results indicate that the density of the CO_2 can strongly influence the jet breakup. Part of the density effect is due to inertial forces. However, the effect of toluene transfer into the CO_2-rich phase is likely to be more significant given that inertial forces did not change morphology for densities from 0.86 to 0.4 g/cm^3. Since toluene is not very soluble in the CO_2 vapor phase (<1%), the jet's viscosity will not be increased significantly. Then, natural and elastic instabilities will be able to grow before polymer vitrification, leading to jet breakup and droplet formation. Finally, it could be expected that the CO_2, which was predissolved in the polymer solution prior to spraying, would assist the breakup of the liquid jet into smaller droplets and may explain in part the small microsphere sizes obtained.

Conclusions

Precipitation with a compressed fluid antisolvent (PCA) is a novel and interesting spray technique for producing a wide variety of polymer microspheres and fibers in a controllable manner. Microspheres, ranging in size from 100 nm to 20 μm, may be formed by adjusting the antisolvent temperature and density. At CO_2 densities greater than ~0.7 g/cm^3 and temperatures below 30°C, extremely small, uniform microspheres are formed, approximately 100 nm in diameter. Because of the low interfacial tensions and large inertial forces, the liquid jet atomizes rapidly, resulting in small droplets. These small droplets lead to even smaller polymer microparticles which are preserved by rapid vitrification as the polymer-rich particles enter the glassy region, due to the large mass-transfer driving forces.

Increasing temperature from 0 to 40°C (at CO_2 densities >0.4 g/cm^3) appears to play an important role by decreasing flocculation and increasing particle size through agglomeration. Polystyrene plasticization by CO_2 is significant at a temperature of 40°C or greater. Density, through a complex mechanism, affects both jet breakup and mass transfer of CO_2 and toluene. In the high-density region, the resultant particles are small microspheres (0.1–1 μm) with some flocculation and agglomeration. At lower densities, the PCA technique becomes more like spray drying with reduced toluene mass-transfer rates. Here, the polymer microspheres are larger and more agglomerated.

At a higher polymer concentration of 5%, the increased viscosity stabilizes the liquid jet and the rapid toluene mass transfer further raises viscosity. Consequently, precipitation and vitrification occur before the jet breaks up, resulting in fibers. Adding small amounts of CO_2 into the polymer solution prior to spraying produces fibers with micropores. Finally, nonporous and porous microspheres can be produced by adding CO_2 to a polymer solution, with diameters from 1 to ~100 μm.

In both the PCA and RESS processes, uniform submicron microspheres can be formed. Both processes utilize the compressible nature of the fluid to control particle morphology and size advantageously. A primary advantage of RESS is that an organic solvent may not be needed, whereas for PCA polymer solubilities are higher and pressures are lower.

Acknowledgment

Acknowledgment is made to Ramzi Abukadra for graciously providing polystyrene microspheres made by emulsion polymerization. We also thank Gabriel Luna-Bárcenas, Don Paul, Bill Koros, and Robert Schechter for many helpful discussions. Finally, acknowledgment is made to the Separations Research Program at the University of Texas, the State of Texas Energy Research in Applications Program, and the Camille and Henry Dreyfus Foundation for a Teacher-Scholar Grant (to KPJ).

Notation

C = constant
D = diameter of drop of liquid
d = jet diameter
L = jet breakup length
N_{Re} = Reynolds number (dimensionless)
N_{We} = Weber number (dimensionless)
V = relative velocity between flowing liquid jet and CO_2
Z = Ohnesorge number (dimensionless)
ρ_A = density of fluid
σ = liquid interfacial tension
μ = jet viscosity

Literature Cited

Aubert, J. H., and R. L. Clough, "Low-Density, Microcellular Polystyrene Foams," *Polym.*, **26**, 2047 (1985).

Aubert, J. H., and A. P. Sylwester, "Microcellular Foams? Here's How!," *Chemtech*, 290 (May, 1991).

Berens, A. R., and G. S. Huvard, "Interaction of Polymers with Near-Critical Carbon Dioxide," *Amer. Chem. Soc. Symp. Ser.*, No. 406, 207 (1989).

Billmeyer, F. W., Jr., *Textbook of Polymer Science*, Wiley, New York (1984).

Bird, R. B., R. C. Armstrong, and O. Hassager, *Dynamics of Polymeric Liquids: 1. Fluid Mechanics*, Wiley, New York (1977).

Burkholder, H. C., and J. C. Berg, "Effect of Mass Transfer on Laminar Jet Breakup: I. Liquid Jets in Gases; II. Liquid Jets in Liquids," *AIChE J.*, **20**, 863 (1974).

Chang, C. J., and A. D. Randolph, "Solvent Expansion and Solute Solubility Predictions in Gas-Expanded Liquid," *AIChE J.*, **36**, 939 (1990).

Chen, S. J., and M. Radosz, "High-Pressure Phase Equilibria in Binary and Ternary Systems of Alternating Poly(Ethylene-Propylene)," Int. Symp. on Supercritical Fluids, Boston (May 20–22, 1991).

Chiou, J. S., J. W. Barlow, and D. R. Paul, "Plasticization of Glassy Polymers by CO_2," *J. Appl. Polym. Sci.*, **30**, 2633 (1985).

Colton, J. S., and N. P. Suh, "The Nucleation of Microcellular Thermoplastic Foam with Additives: Part II: Experimental Results and Discussion," *Polym. Eng. Sci.*, **27**, 493 (1987).

Condo, P. D., I. C. Sanchez, C. G. Panayiotou, and K. P. Johnston, "Glass Transition Behavior Including Retrograde Vitrification of Polymers with Compressed Fluid Diluents," *Macromolecules*, **25**, 6119 (1992).

Coyle, R. W., J. C. Berg, and J. C. Niwa, "Liquid-Liquid Jet Breakup Under Conditions of Relative Motion, Mass Transfer and Solute Adsorption," *Chem. Eng. Sci.*, **36**, 19 (1981).

Daneshvar, M., and E. Gulari, "Partition Coefficients of Poly(ethylene glycol)s in Supercritical Carbon Dioxide," *Amer. Chem. Soc. Symp. Ser.*, No. 406, 72 (1989).

Debenedetti, P. G., "Homogeneous Nucleation in Supercritical Fluids," *AIChE J.*, **36**, 1289 (1990).
Dixon, D. J., and K. P. Johnston, "Molecular Thermodynamics of Solubilities in Gas Antisolvent Crystallization," *AIChE J.*, **37**, 1441 (1991).
Fleming, G. K., and W. J. Koros, "Dilation of Polymers by Sorption of Carbon Dioxide at Elevated Pressures: 1. Silicone Rubber and Unconditioned Polycarbonate," *Macromolecules*, **19**, 2285 (1986).
Francis, A. W., "Ternary Systems of Liquid Carbon Dioxide," *J. Phys. Chem.*, **58**, 1099 (1954).
Gallagher, P. M., M. P. Coffey, V. J. Krukonis, and N. Klasutis, "Gas Antisolvent Recrystallization: New Process To Recrystallize Compounds Insoluble in Supercritical Fluids," *Amer. Chem. Soc. Symp. Ser.*, No. 406 (1989).
Garg, A., L. Gerhardt, and E. Gulari, "Solubility of Supercritical Gases in Polydimethylsiloxane," *Int. Symp. on Supercritical Fluids*, Boston (May 20-22, 1991).
Grant, R. P., and S. Middleman, "Newtonian Jet Stability," *AIChE J.*, **12**, 669 (1966).
Heller, J. P., D. K. Dandge, R. J. Card, and L. G. Donaruma, "Direct Thickeners for Mobility Control of CO2 Floods," *Soc. Petroleum Eng. J.*, 679 (Oct., 1985).
Hiemenz, P. C., *Principles of Colloid & Surface Chemistry*, Marcel Dekker, New York (1986).
Johnston, K. P., G. J. McFann, and R. M. Lemert, "Pressure Tuning of Reverse Micelles for Adjustable Solvation of Hydrophiles in Supercritical Fluids," *Amer. Chem. Soc. Symp. Ser.*, No. 406 (1989).
Koenhen, D. M., M. H. V. Mulder, and C. A. Smolders, "Phase Separation Phenomena During the Formation of Asymmetric Membranes," *J. Appl. Polym. Sci.*, **21**, 199 (1977).
Kroesser, F. W., and S. Middleman, "Viscoelastic Jet Stability," *AIChE J.*, **15**, 383 (1969).
Krukonis, V. J., "Supercritical Fluid Nucleation of Difficult-to-Comminute Solids," paper 140f, AIChE meeting, San Francisco (Nov., 1984).
Kumar, S. K., and K. P. Johnston, "Modelling the Solubility of Solids in Supercritical Fluids with Density as the Independent Variable," *J. Supercritical Fluids*, **1**, 15 (1988).
Lee, C., K. L. Hoy, and M. D. Donohue, "Supercritical Fluids as Diluents in Liquid Spray Application of Coatings," U.S. Patent 4,923,720 (1990).
Lefebvre, A. H., *Atomization and Sprays*, Hemisphere Publishing, New York (1989).
Lele, A. K., and A. D. Shine, "Morphology of Polymers Precipitated from a Supercritical Solvent," *AIChE J.*, **38**, 742 (1992).
Lemert, R. M., R. A. Fuller, and K. P. Johnston, "Reverse Micelles in Supercritical Fluids: 3. Amino Acid Solubilization in Ethane and Propane," *J. Phys. Chem.*, **94**, 6021 (1990).
Lloyd, D. R., K. E. Kinzer, and H. S. Tseng, "Microporous Membrane Formation Via Thermally Induced Phase Separation: I. Solid-Liquid Phase Separation," *J. Memb. Sci.*, **52**, 239 (1990).
Lloyd, D. R., S. S. Kim, and K. E. Kinzer, "Microporous Membrane Formation Via Thermally Induced Phase Separation: II. Liquid-Liquid Phase Separation," *J. Memb. Sci.*, **64**, 1 (1991).
Matson, D. W., J. L. Fulton, R. C. Petersen, and R. D. Smith, "Rapid Expansion of Supercritical Fluid Solutions: Solute Formation of Powders, Thin Films, and Fibers," *Ind. Eng. Chem. Res.*, **26**, 2298 (1987).
McHugh, M. A., and T. L. Guckes, "Separating Polymer Solutions with Supercritical Fluids," *Macromolecules*, **18**, 674 (1985).
McHugh, M. A., and V. J. Krukonis, *Supercritical Fluid Extraction Principles and Practice*, Butterworths, Stoneham, MA (1986).
Meilchen, M. A., B. M. Hasch, and M. A. McHugh, "Effect of Copolymer Composition on the Phase Behavior of Mixtures of Poly(ethylene-co-methyl acrylate) with Propane and Chlorodifluoromethane," *Macromolecules*, **24**, 4874 (1991).
Müller, B. W., and W. Fischer, "Manufacture of Sterile Sustained-Release Drug Formulations Using Liquified Gases," Germany Patent Application DE 3,744,329 A1 (1989).
Napper, D. H., *Polymeric Stabilization of Colloidal Dispersions*, Academic Press, New York (1983).
Nauman, E. B., M. V. Ariyapadi, N. P. Balsara, T. A. Grocela, J. S. Furno, S. H. Liu, and R. Mallikarjun, "Compositional Quenching: A Process for Forming Polymer-In-Polymer Microdispersions and Cocontinuous Networks," *Chem. Eng. Comm.*, **66**, 29 (1988).
Ng, H. J., and D. B. Robinson, "Equilibrium Phase Properties of the Toluene-Carbon Dioxide System," *J. Chem. Eng. Data*, **24**, 325 (1978).
O'Sullivan, D., "New Propellant System Devised for Aerosol Packaging," *C&EN*, 13 (Jan., 1992).
Petersen, R. C., D. W. Matson, and R. D. Smith, "The Formation of Polymer Fibers From the Rapid Expansion of Supercritical Fluid Solutions," *Polym. Eng. Sci.*, **27**, 1693 (1987).
Pinnau, I., "Skin Formation of Integral-Asymmetric Gas Separation Membranes Made by Dry-Wet Phase Inversion," PhD Thesis, Univ. of Texas at Austin (1991).
Rangarajan, B., and C. T. Lira, "Production of Aerogels," *J. Supercritical Fluids*, **4**, 1 (1991).
Seckner, A. J., A. K. McClellan, and M. A. McHugh, "High-Pressure Solution Behavior of the Polystyrene-Toluene-Ethane System," *AIChE J.*, **34**, 9 (1988).
Shim, J., and K. P. Johnston, "Adjustable Solute Distribution Between Polymers and Supercritical Fluids," *AIChE J.*, **35**, 1097 (1989).
Shim, J., and K. P. Johnston, "Molecular Thermodynamics of Solute-Polymer-Supercritical Fluid Systems," *AIChE J.*, **37**, 607 (1991b).
Shim, J., and K. P. Johnston, "Phase Equilibria, Partial Molar Enthalpies, and Partial Molar Volumes Determined by Supercritical Fluid Chromatography," *J. Phys. Chem.*, **95**, 353 (1991a).
Tom, J. W., and P. G. Debenedetti, "Formation of Bioerodible Polymeric Microspheres and Microparticles by Rapid Expansion of Supercritical Solutions," *Biotechnol. Prog.*, **7**, 403 (1991a).
Tom, J. W., and P. G. Debenedetti, "Particle Formation with Supercritical Fluids—A Review," *J. Aerosol Sci.*, **22**, 555 (1991b).
Tsai, F., and J. M. Torkelson, "Roles of Phase Separation Mechanism and Coarsening in the Formation of Poly(methyl methacrylate) Asymmetric Membranes," *Macromolecules*, **23**, 775 (1990).
Tsay, C. S., and A. J. McHugh, "Mass Transfer Modeling of Asymmetric Membrane Formation by Phase Inversion," *J. Polym. Sci.: Part B: Polym. Phys.*, **28**, 1327 (1990).
Watkins, J. J., V. J. Krukonis, P. D. Condo, Jr., D. Pradhan, and P. Ehrlich, "Fractionation of High Density Polyethylene in Propane by Isothermal Pressure Profiling and Isobaric Temperature Profiling," *J. Supercritical Fluids*, **4**, 24 (1991).
Wissinger, R. G., and M. E. Paulaitis, "Glass Transitions in Polymer-CO2 Mixtures at Elevated Pressures," *J. Polym. Sci., Part B, Polym. Phys.*, **29**, 631 (1991a).
Wissinger, R. G., and M. E. Paulaitis, "Molecular Thermodynamic Model for Sorption and Swelling in Glassy Polymer-CO2 Systems at Elevated Pressures," *Ind. Eng. Chem. Res.*, **30**, 842 (1991b).
Yilmaz, L., and A. J. McHugh, "Analysis of Nonsolvent-Solvent-Polymer Phase Diagrams and Their Relevance to Membrane Formation Modeling," *J. Appl. Polym. Sci.*, **31**, 997 (1986).

Manuscript received May 1, 1992, and revision received Aug. 4, 1992.